J Cell Sci. 2010 Jul 20;123(16):2763–2772. doi: 10.1242/jcs.066589

The *Drosophila* SUN protein Spag4 cooperates with the coiled-coil protein Yuri Gagarin to maintain association of the basal body and spermatid nucleus

Martin P Kracklauer [1,2], Heather M Wiora [1,*], William J Deery [3], Xin Chen [4,‡], Benjamin Bolival Jr [4], Dwight Romanowicz [1], Rebecca A Simonette [3], Margaret T Fuller [4], Janice A Fischer [1], Kathleen M Beckingham [3,§]

Author information Article notes Copyright and License information

PMCID: PMC2915878 PMID: 20647369

Abstract

Maintaining the proximity of centrosomes to nuclei is important in several cellular contexts, and LINC complexes formed by SUN and KASH proteins are crucial in this process. Here, we characterize the presumed *Drosophila* ortholog of the mammalian SUN protein, sperm-associated antigen 4 (Spag4, previously named Giacomo), and demonstrate that Spag4 is required for centriole and nuclear attachment during spermatogenesis. Production of *spag4* mRNA is limited to the testis, and Spag4 protein shows a dynamic pattern of association with the germline nuclei, including a concentration of protein at the site of attachment of the single spermatid centriole. In the absence of Spag4, nuclei and centrioles or basal bodies (BBs) dissociate from each other after meiosis. This role of Spag4 in centriolar attachment does not involve either of the two KASH proteins of the *Drosophila* genome (Klarsicht and MSP-300), but does require the coiled-coil protein Yuri Gagarin. Yuri shows an identical pattern of localization at the nuclear surface to Spag4 during spermatogenesis, and epistasis studies show that the activities of Yuri and dynein-dynactin are downstream of *spag4* in this centriole attachment pathway. The later defects in spermatogenesis seen for *yuri* and *spag4* mutants are similar,

suggesting they could be secondary to initial disruption of events at the nuclear surface.

Keywords: KASH protein, SUN protein, Centrosome, Centriole, Coiled-coil proteins, Sperm basal body, Spermatogenesis

Introduction

Within eukaryotic cells, a centrosome or spindle-pole body (SPB) functions as a microtubule-organizing center (MTOC) and is typically found closely apposed to the nuclear membrane. Disruption of the MTOC-nucleus association frequently leads to cellular abnormalities, including defective nuclear positioning (Malone et al., 1999; Starr et al., 2001), abnormal morphology of cells and organelles (Fischer-Vize and Mosley, 1994; Mosley-Bishop et al., 1999; Patterson et al., 2004), altered cell migration (Gomes et al., 2005; Lüke et al., 2008) and defective chromosome segregation during mitosis (Malone et al., 2003; Xiong et al., 2008). These findings indicate that the nuclear-MTOC association is essential in many cellular processes.

Nuclear-MTOC association is often maintained by a LINC complex comprising SUN (Sad1/UNC) and KASH (Klar-ANC-Syne homology) proteins (Gruenbaum et al., 2005; Starr and Fischer, 2005; Crisp et al., 2006; Stewart-Hutchinson et al., 2008). SUN and KASH proteins are integral membrane proteins of the inner and outer nuclear membranes (INM and ONM), respectively. These proteins interact with each other in the intermembrane space via their C-terminal SUN and KASH domains (McGee et al., 2006; Kracklauer et al., 2007). The N-terminal domains of SUN proteins face the nucleoplasmic side of the INM, interacting with the nuclear lamina or with chromatin (Bray et al., 2002; Hodzic et al., 2004; King et al., 2008; Xiong et al., 2008). N-terminal domains of KASH proteins typically face the cytoplasm, and interact with components of the actin or microtubule filament systems (Starr and Han, 2002; Zhang et al., 2002; Fischer et al., 2004; Wilhelmsen et al., 2005; Ketema et al., 2007). A detailed model for the mechanism by which the *Caenorhabditis elegans* KASH protein ZYG-12 links the zygotic centrosome to the nuclear envelope (NE) has been proposed (Malone et al., 2003), which involves direct interaction of certain ZYG-12 isoforms with the microtubule motor dynein.

The *Drosophila* genome encodes two KASH protein genes, *klarsicht* (Mosley-Bishop et al., 1999) and *msp-300* (Zhang et al., 2002) and two SUN protein genes, *klaroid* (Kracklauer et al., 2007) and gene *CG6589*. *CG6589*, previously termed *giacomo*, has proved to have sequence homology to the testis-specific mammalian SUN protein Spag4 (Shao et al., 1999; Kennedy et al., 2004) (supplementary material Fig. S1) and thus we have re-named the gene *spag4*. We show here that Spag4 has a crucial role in spermatogenesis comparable to that of other SUN proteins: it is necessary for anchoring the centriole or basal body (BB) to the spermatid nucleus. But surprisingly, this role does not require formation of a typical LINC complex with a KASH protein. Instead, we have shown that the coiled-coil cytoplasmic protein Yuri Gagarin (Armstrong et al., 2006; Texada et al., 2008) is an essential component of the Spag4-BB anchoring mechanism, and that regulation of dynein-dynactin localization by Spag4 has a role in the process.

Results

Spliced *spag4* mRNA is found only in testes and encodes a transmembrane domain protein

We first analyzed the expression of *spag4* mRNA by RT-PCR, and observed that spliced mRNA is found only in male larvae, pupae and adults (Fig. 1A), suggesting testis-specific expression. Expression of *spag4* mRNA characterized at www.flyatlas.org confirms this testis specificity. In situ hybridization demonstrated that *spag4* mRNA expression peaks in the early primary spermatocyte region of adult testes (Fig. 1B). Low levels of the unspliced precursor transcript were observed in females (Fig. 1A), but appear to be functionless given the viability and fertility of *spag4*-null females (see below).

Fig. 1.

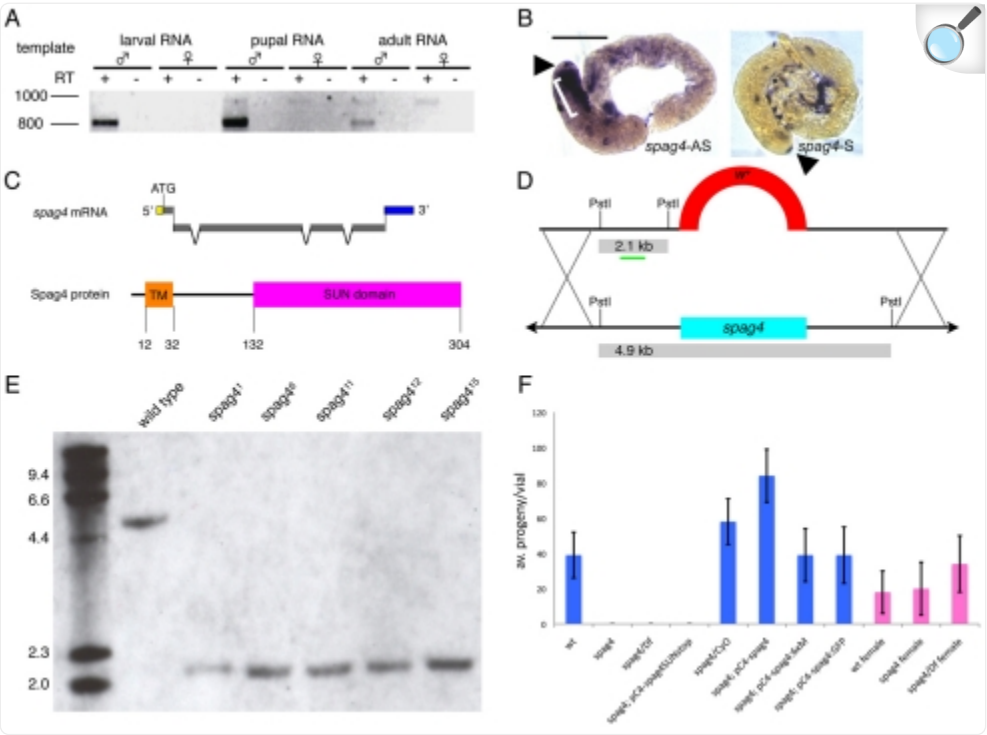

Open in a new tab

***spag4* expression, *spag4* knockout and fertility assays.** (**A**) *spag4* mRNA (~800bp) is limited to males, but low levels of the primary transcript (~1000 bp) are present in male and female pupae and adults. (**B**) *spag4* mRNA localization in wild-type testes by ISH. AS, antisense; S, sense probe control. Scale bar: 200 μm. White bracket: region of *spag4* mRNA expression. Arrowheads indicate apical tips of testes. (**C**) Schematics (relatively proportional but not to scale) of *spag4* transcription unit determined by 5′RLM-RACE and 3′RACE, and Spag4 protein and its domains. Newly identified regions of transcription unit are shown. Yellow and blue indicate 5′ and 3′ UTR, respectively. Amino acid boundaries of the TM and SUN domains are shown below. (**D**) Ends-out homologous recombination scheme for deletion of *spag4*. Gray bars: *PstI* fragments of wild-type (bottom strand) and mutant (top strand) DNA detected by Southern blot probe (green bar). The mini-white (w^+) gene replaces *spag4* upon recombination. (**E**) Genomic Southern blots of *PstI*-digested DNA from wild-type flies and the five *spag4*-null mutants isolated. *PstI* fragments and probe as in D. (**F**) Fertility assays for *spag4*-related lines. Error bars indicate s.d.; *n*=20 for each genotype. Blue bars, males; pink bars, females.

Although all SUN proteins described to date have a transmembrane (TM) domain N-terminal to the SUN domain

(Hagan and Yanagida, 1995; Malone et al., 1999; Shao et al., 1999; Dreger et al., 2001; Malone et al., 2003; Hodzic et al., 2004; Kracklauer et al., 2007; Liu et al., 2007), the originally annotated Spag4 protein sequence contains no TM domain (Tweedie et al., 2009). Using 5′ RNA-ligase-mediated rapid amplification of cDNA ends (RLM-RACE), we identified 5′ *spag4* mRNA sequences encoding an N-terminus with a single TM helix (Fig. 1C). 3′ RACE also revealed a previously uncharacterized 3′ UTR. The corrected *spag4* gene region spans ~1.2 kb of genomic DNA (Fig. 1C).

spag4 mutant males are sterile

To determine the function of *spag4*, we generated knockout mutations by ends-out homologous recombination (Fig. 1D,E, and Materials and Methods). Homozygous mutant individuals developed normally, yielding adults that were wild type in appearance. However, mutant males [either homozygous or in *trans* to deficiency *Df(2L)Prl*] were completely sterile (Fig. 1F). *spag4*-null males courted, mounted and copulated with females (data not shown), suggesting that male sterility is not a behavioral defect. Mutant females were fertile, consistent with a lack of *spag4* mRNA splicing in females. Male fertility was restored to *spag4* mutants by introducing a single copy of a 4.9 kb genomic *spag4* transgene (Fig. 1F and supplementary material Fig. S3). A transgene generating Spag4 protein lacking the SUN domain (supplementary material Fig. S3) did not restore fertility to *spag4*-null males (Fig. 1F), indicating that Spag4 requires this domain for its role in spermatogenesis.

Dynamic Spag4 subcellular localization during gametogenesis

To address how Spag4 contributes to male gametogenesis, we examined protein localization in the testis using flies expressing Spag4 tagged C-terminally with 6×MYC or GFP. Transgenes similar to the *spag4* rescue construct containing these tags (supplementary material Fig. S3) restored fertility to *spag4* males, indicating that the tagged genes have wild-type function and that the tagged proteins are likely to localize normally. All independent insertions of both transgenes produced identical localization patterns. In general, Spag4:6×MYC gave stronger signals, but for mature sperm in the seminal vesicle, the Spag4:GFP signal was more robust (Fig. 2J). Most data shown here derives from Spag4:6×MYC.

Fig. 2.

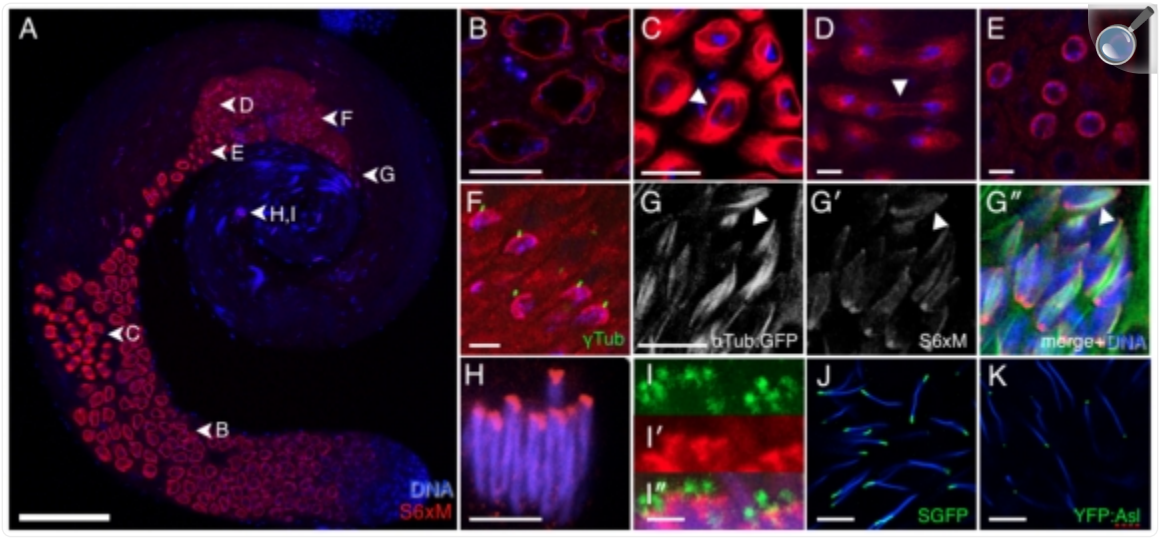

Open in a new tab

Dynamic localization of Spag4 during spermatogenesis. (**A**) Whole-mount testis (excluding seminal vesicle) expressing Spag4:6×MYC. Lettered arrowheads indicate approximate regions where data in the other panels were obtained. NE localization in polar and mature primary spermatocytes (**B**) and in round spermatids (**E**). Spindle-associated localization during meiosis I and II (**C**,**D**); arrowheads indicate spindle fibers. Caps of Spag4:6×MYC on late round spermatid nuclei with the centrioles (γ-tubulin stained) at their apices (**F**). Focus of Spag4:6×MYC at centriolar attachment site and along dense complex microtubules (e.g. arrowhead) in early elongating spermatids (**G-G″**). A concentration of Spag4:6×MYC at the apical tip of elongating spermatid nuclei (**H**,**I′**) is shown by the basal body marker YFP:Asl (**I**) to lie between the BB and the nuclei proper (**I″**). This Spag4:6×MYC focus persists on mature sperm in the seminal vesicle (**J**), similarly to the BB marker YFP:Asl (**K**). Red, Spag4:6×MYC; blue, DAPI; green, γ-tubulin in F, α-Tub:GFP in G″, YFP:Asl in I and K, Spag4:GFP in J. Scale bars: 150 μm (A), 20 μm (B-G,J,K) and 10 μm (H,I).

In the *Drosophila* testis, germ cells are arranged in a spatio-temporal order, from the apical tip to the basal seminal vesicle. Consistent with the in situ hybridization results, Spag4:6×MYC was not detectable at the apical tip, where germ-line stem cells and spermatogonia reside (Fig. 1B, Fig. 2A). Four rounds of synchronous divisions yield 16 interconnected spermatogonia, encapsulated in a cyst. These spermatogonia become spermatocytes and commit to meiosis, resulting in 64 interconnected round spermatids. Spag4:6×MYC was first detected in primary spermatocytes where it was associated closely with the NE, as demonstrated by colocalization with lamin (supplementary material Fig. S4D-F). Spag4:6×MYC remained at the NE as nuclei became grooved and lobular during primary spermatocyte growth

(Fig. 2B). Upon NE breakdown, Spag4:6×MYC colocalized with subsets of microtubules in the meiosis I spindles (Fig. 2C; supplementary material Fig. S4A-C), and possibly the parafusorial membranes (Fuller, 1993). In late meiosis II, Spag4:6×MYC again associated with spindle microtubules (supplementary material Fig. S4A′-C′) cupping the astral region of re-forming nuclei (Fig. 2D). As post-meiotic round spermatids formed, Spag4:6×MYC once again localized to the NE (Fig. 2E).

Once meiosis is complete, the single centriole of each round spermatid attaches to its nuclear surface, and dramatic morphological changes commence. The centriole differentiates into the BB, from which the axoneme develops, and the nuclei elongate and condense to a needle-like shape. The Spag4:6×MYC protein at the NE initially transformed into a hemispherical cap (the 'cap') with the centriole at its apex (Fig. 2F). Subsequently, on the elongating nuclei, Spag4:6×MYC assumed a two-component pattern, with a focus of the protein at the centriole or BB attachment site, and a stripe of protein along the long axis of the nuclei (the 'stripe'). From EM studies, Tokuyasu (Tokuyasu, 1974) identified electron-dense material, termed the dense complex, which initially formed as a pericentriolar hemispherical cap on round spermatid nuclei and was later present as a stripe rich in microtubules along the length of the elongating nuclei. That the stripe of Spag4:6×MYC is at the position of the dense complex was established by colocalization in testes expressing α-tubulin:GFP (Fig. 2G-G″). As elongation proceeded, the Spag4:6×MYC stripe along the dense complex gradually disappeared, and the focus at the BB became more compact and assumed a distinctive trefoil or bell shape (Fig. 2H). As shown by colocalization with the pancentriolar marker YFP:Asl (Varmark et al., 2007) (Fig. 2I-I″), this focus of Spag4 protein was between the caudal nuclear tip and BB, thus placing it at the ~0.5 μm indentation (the 'dent') in the nucleus in which the BB sits (Tokuyasu, 1975). Spag4:GFP persisted on sperm nuclei in the seminal vesicle (Fig. 2J), as did YFP:Asl (Fig. 2K), suggesting that Spag4 remains at the BB attachment site in mature sperm.

This dynamic pattern of Spag4 localization is unusual; other SUN proteins localize specifically to the NE (Malone et al., 1999; Malone et al., 2003; Hodzic et al., 2004; Kracklauer et al., 2007; Liu et al., 2007), microtubules (Shao et al., 1999) or the MTOC or SPB (Hagan and Yanagida, 1995; Xiong et al., 2008). However, this range of localizations for Spag4 might be more a property of the developmental process in question rather than the protein. So far, other SUN proteins have been studied in less complex developmental situations.

The initial defect in *spag4* mutant males is failure of centriole-nuclear attachment

To address the role of Spag4 during sperm development, we analyzed spermatogenesis in the *spag4*-null mutant. Our goal was to identify the first detectable defects caused by the mutation, because later problems might be secondary to these initial failures. Despite the association of Spag4 with the NE of the primary spermatocyte, in the *spag4* mutant, the primary spermatocyte stage appeared similar to the wild type (Fig. 3A,D). However, beginning in the round spermatid stage, some disruption of the centriole linkage was detectable (Fig. 3B,E), which became pronounced and fully penetrant as the nuclei condensed and elongated. In contrast to the wild type (Fig. 3C), in all elongate *spag4* mutant nuclear bundles examined, BBs labelled with YFP:Asl had lost their normal association with the caudal nuclear tips and

were scattered along the nuclear bundles (NBs) (Fig. 3G). Furthermore, every NB observed showed some degree of dispersion within the cysts, and the scattered nuclei frequently curled in the terminal region of the testis (Fig. 3H). These findings indicate that Spag4 is required to maintain the correct centriole-nuclear association, and has a role in shaping elongated nuclei.

Fig. 3.

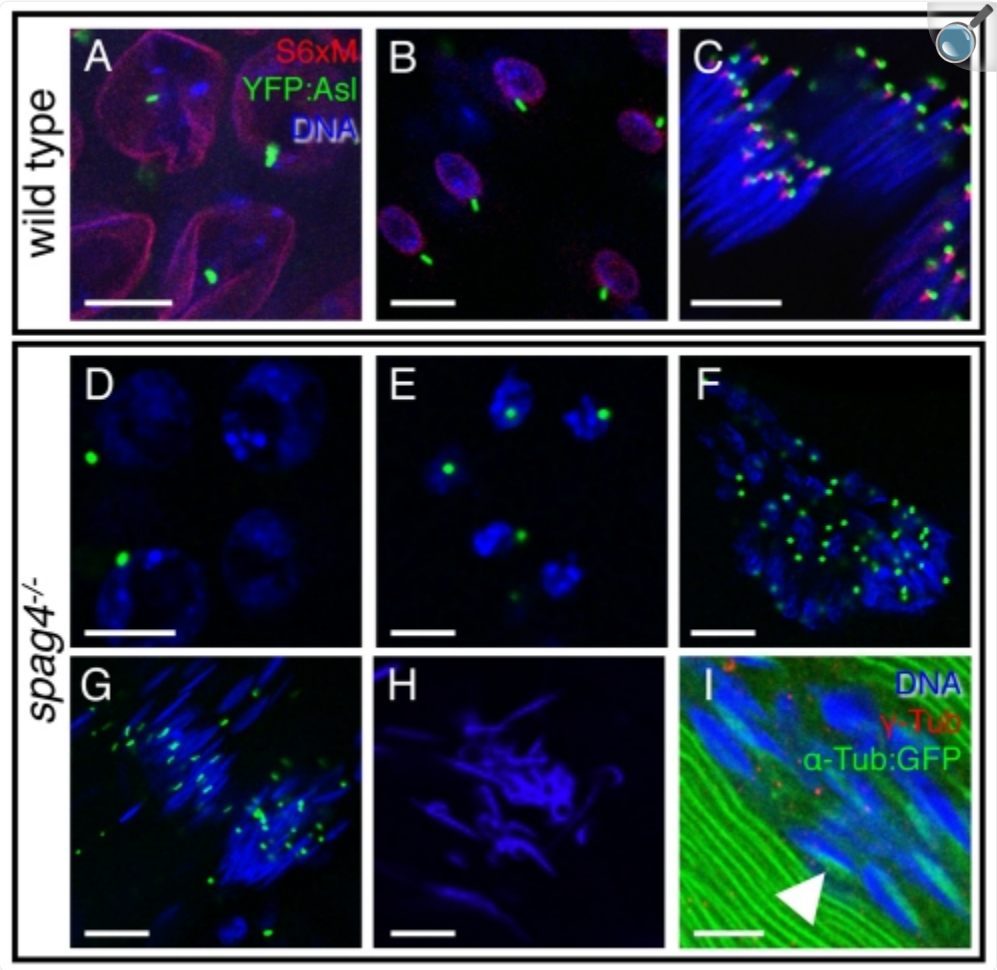

Open in a new tab

Nuclear-centriolar dissociation during elongation stages is the earliest visible defect in *spag4* mutant testes. Centriolar association with primary spermatocyte (**A**), round spermatid (**B**) and elongating (**C**) nuclei in wild-type testes. In *spag4* mutant testes, centriolar association is normal in primary spermatocytes (**D**) and mostly normal in round spermatids (**E**), and early elongating spermatids (**F**). (**G**) Fully penetrant nuclear-centriolar dissociation becomes apparent in later elongation stages. (**H**) Nuclei contort in advanced elongation stages. (**I**) The microtubules of the dense complex stripe are retained on *spag4* spermatid nuclei. Scale bars: 20 μm (A,D), 10 μm (B,C,E,I) and 15 μm (F,G,H).

Later defects in *spag4* mutant spermatogenesis

In wild-type males, the seminal vesicle fills with mature sperm after several days of sequestration away from females. By contrast, no mature sperm accumulated in the seminal vesicles of sequestered *spag4* mutant males (supplementary material Fig. S5), suggesting that developmental processes subsequent to BB-nuclear interaction also fail in the mutant. We thus investigated events during individualization, the process immediately following elongation. During individualization, elongated, syncytially connected spermatids are separated into individual sperm. An individualization complex (IC) composed of 64 actin cones that assemble around individual sperm nuclei forms, and then moves along the cyst towards the caudal ends of the spermatids (Hicks et al., 1999; Noguchi and Miller, 2003; Noguchi et al., 2008). As the IC moves along the cyst, each spermatid becomes surrounded by plasma membrane, and excess cytoplasm is pushed as a cytoplasmic bulge to the caudal tip of the cyst to form a 'waste bag'. Using TEM to analyze cross-sections of testes, we found that *spag4* mutants had defective individualization. In the wild type, cross-sections reveal an iterative pattern of individualized spermatids, each with a single axoneme and major and minor mitochondrial derivative (MD) surrounded by plasma membrane (Fig. 4D). In *spag4* mutant cysts, arrays of axonemes each associated with a single major and minor MD were also seen (Fig. 4E). Furthermore, although axoneme structure was not analyzed in detail, it appeared grossly normal, with a small number of axonemes lacking the central microtubule doublets (typically less than 10 axonemes/cyst). However, both MDs showed failure to condense fully, a problem that was most marked for the minor MD. But most strikingly, plasma membrane investment largely failed to occur (Fig. 4D,E) and copious amounts of cytoplasm remained in the mutant cysts (Fig. 4E). Thus, sperm individualization and cytoplasmic elimination are severely affected in the *spag4* mutant.

Fig. 4.

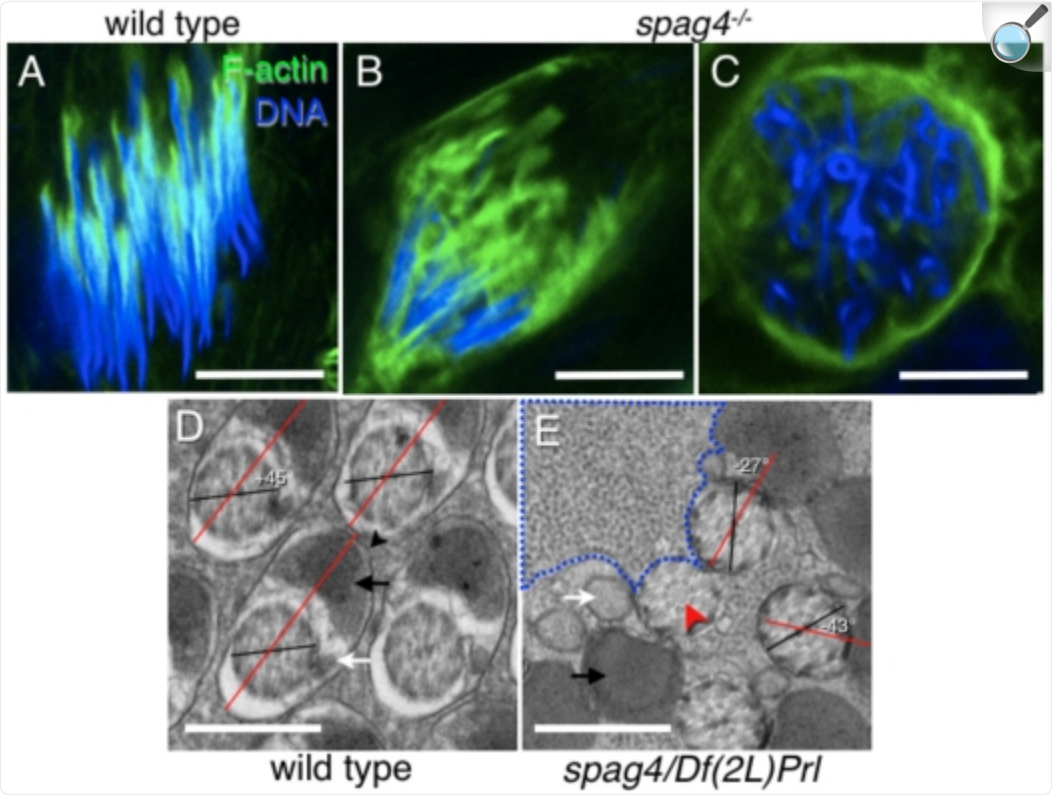

Open in a new tab

Individualization fails in the *spag4* mutant testes. (**A**) Normal actin cones of the individualization complex (IC) form on wild-type elongated nuclei. (**B**) Abnormal actin deposition forms aberrant ICs in the *spag4* mutant. (**C**) Lack of actin deposition on curled nuclei in the *spag4* mutant. (**D**) TEM of wild-type elongated cyst cross-section. Black lines denote axis through the central doublet of the axoneme; within a wild-type cyst, spermatid cross-sections (red lines) lie at a constant angle (clockwise 45° to the central doublet. (**E**) In *spag4* mutant cysts, aberrant angles demonstrate spermatid-axoneme misalignment. Red arrowhead indicates missing central doublet in *spag4* axoneme. Images in D and E were taken in comparable regions of wild-type and mutant testes (towards terminal epithelium, immediately apical to cyst coiling region). Black arrows indicate major mitochondrial derivatives (MDs) and white arrows, minor MDs. Black arrowhead in D indicates plasma membrane. Both major and minor MDs are less condensed in *spag4* mutant than in the wild type, and large regions of ribosome-rich cytoplasm persist in the cysts (blue dotted line). Scale bars: ~10 μm (A-C), 500 nm (D,E).

A spatially controlled caspase cascade used in a non-apoptotic context promotes spermatid individualization (Huh et al.,

2004; Muro et al., 2006). We found that caspase activation, as monitored with an antibody (anti-CM1) that recognizes the active form of the *Drosophila* effector caspase Ice (Arama et al., 2003; Muro et al., 2006; Zhong and Belote, 2007), was similar in *spag4* mutant and wild-type testes (supplementary material Fig. S6A-B′). Successful activation of caspase was further confirmed by staining testes with Acridine Orange, a dye taken up by cysts undergoing individualization. (supplementary material Fig. S6A″,B″) (Arama and Steller, 2006). Thus, defective individualization in the mutant is not due to defective caspase activation. Instead, the defects appear to originate in aberrant formation of ICs. In the *spag4* mutant, the individual actin cones were disrupted, with cones no longer forming organized ICs (Fig. 4A,B). In bundles of contorted nuclei, actin cones were often missing altogether (Fig. 4C). The disorganized ICs tended not to progress caudally, and mutant testes lacked cytoplasmic bulges and waste bags, indicating failures in individualization (supplementary material Fig. S6). Despite failed individualization, the elongated syncytial cysts in *spag4* mutants attempted the final coiling process that precedes sperm movement into the seminal vesicle: the terminal region of mutant testes thus filled with coiling cysts (supplementary material Fig. S5D).

Phenotype comparisons suggest interactions with *yuri* and *dynein-dynactin* but not known KASH proteins

spag4 encodes a SUN protein and localizes to the NE during most of spermatogenesis. Furthermore, the SUN domain is essential for the role of *spag4* in male fertility (Fig. 1F). These findings suggest that Spag4 functions as a typical SUN protein, forming a LINC complex with a KASH protein partner. However, our data indicate that neither of the two *Drosophila* KASH proteins (Klarsicht and MSP-300) is a Spag4 partner in the testis. For both genes, mutations that eliminate the KASH domain are available: $msp300^{\Delta KASH}$ was generated by ends-out recombination (Xie and Fischer, 2008) and the $klar^{CD4}$ mutation came from EMS mutagenesis that generated a suitably positioned stop codon (Mosley-Bishop et al., 1999; Fischer et al., 2004; Guo et al., 2005). Mutant males of both genotypes were fertile (Fig. 5A) and in all cysts examined for $msp300^{\Delta KASH}$ males, $klar^{CD4}$ males and $msp300^{\Delta KASH}$; $klar^{CD4}$ double-mutant males, (44-95 cysts in 10 testes per genotype), the centrioles remained associated with the spermatid nuclei during elongation (Fig. 5B-D) and nuclear bundling, IC formation and IC progression were normal. There was no heterozygous effect of the *spag4*-null genotype on the fertility of $klar^{CD4}$ mutant males (Fig. 5A) and the only aberrancy detected in the spermatid cysts of these various genotypes was the occasional apical mislocalization of nuclear bundles in $klar^{CD4}$ and $msp300^{\Delta KASH}$; $klar^{CD4}$ double-mutant males (data not shown). The doubly mutant males were somewhat subfertile (Fig. 5A), but this probably reflects defects in the testis sheath (data not shown) that are not found in the singly mutant males.

Fig. 5.

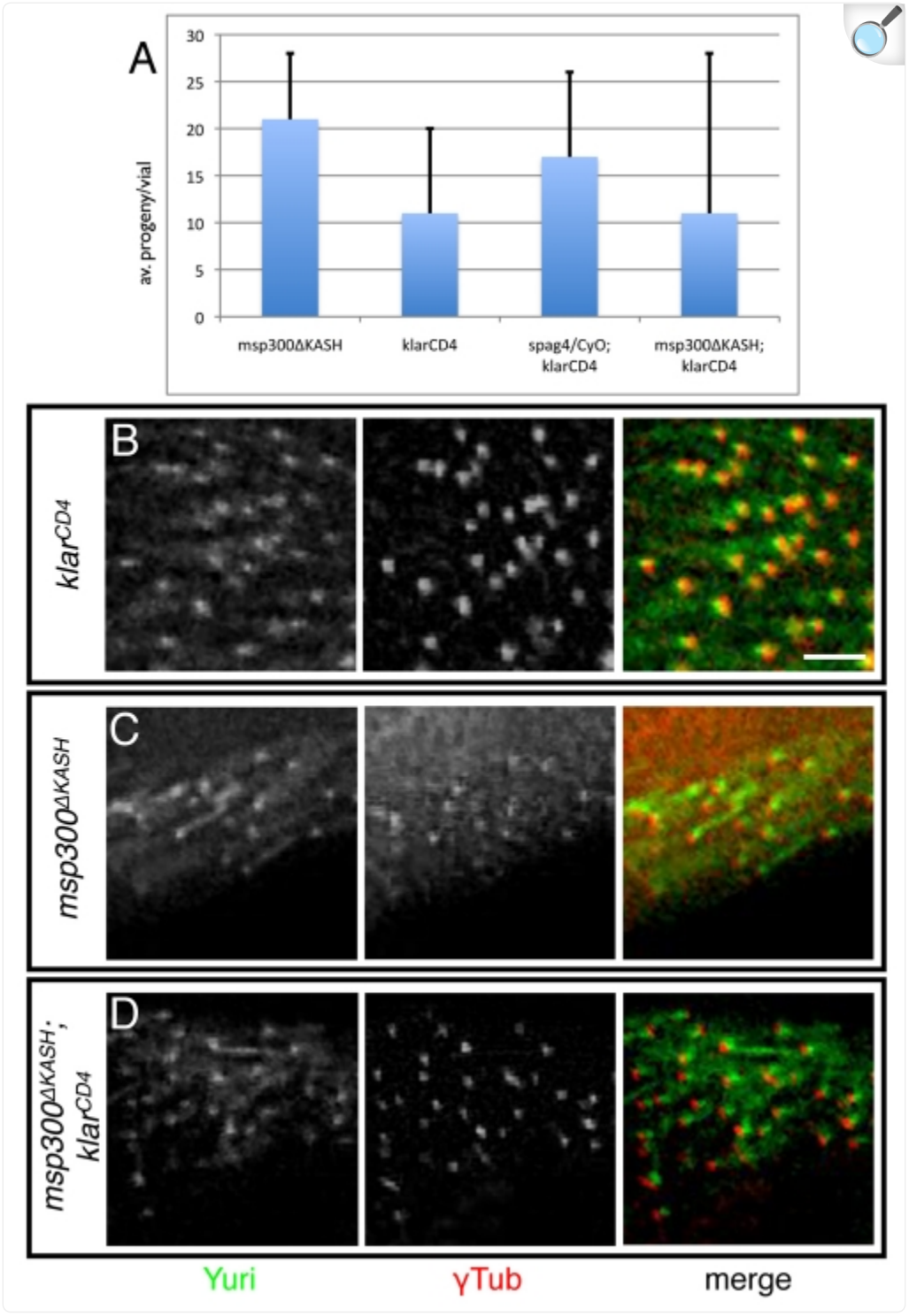

Open in a new tab

Linking the spermatid nucleus to the centriole or BB does not require a KASH domain protein. (**A**) Fertility assays for KASH-domain protein alleles. *n*=20 for each genotype. Error bars indicate s.d. All

genotypes are at least partially fertile. The large error bars in *msp300$^{\Delta KASH}$; klar^{CD4}* double mutants are due to high (40%) male death during the assay. Compare with Fig. 1F for wild-type male fertility levels. Centriolar-nuclear attachment is normal in elongating nuclei bundles from *klar^{CD4}* (**B**), *msp300$^{\Delta KASH}$* (**C**) and *msp300$^{\Delta KASH}$; klar^{CD4}* (**D**) mutant males as shown by tight juxtaposition of γ-tubulin staining (red) of the centriolar adjunct to the dent component of Yuri staining (green, see text, Fig. 6J and supplementary material Fig. S7). Scale bar: 10 μm.

By contrast, both the male sterile phenotype of *spag4* and the post-meiotic localization pattern of Spag4:6×MYC are compellingly similar to findings for a male sterile mutation of the *yuri* locus (*yuri^{F64}*) and for Yuri nuclear localization (Texada et al., 2008). *yuri* is a complex locus encoding three major classes of ubiquitously expressed isoforms. The longer isoforms largely consist of coiled-coil regions. The *yuri^{F64}* mutation eliminates expression of the middle size Yuri isoforms globally, but, uniquely in the testis, the shortest isoform is also not expressed. This loss of two isoforms in the testis might explain the observation that the *yuri^{F64}* mutant exhibits male sterility, but no other developmental phenotype. An antibody that detects all isoforms showed Yuri accumulation in the postmeiotic nuclear cap, dent and stripe patterns exactly as described above for Spag4 and confirmed here by localization (Fig. 5B-D, Fig. 6) and colocalization (supplementary material Fig. S7) studies. In *yuri^{F64}*, this nuclear localization of Yuri was absent and, as in the *spag4*-null, the centrioles lost their normal attachments to the post-meiotic nuclei and the NBs became disorganized, with nuclei forming curled, distorted shapes. Similar defects in late spermatogenesis were also shared by *yuri^{F64}* and *spag4*-null flies, including failure of actin cone formation and individualization, aberrant MD condensation, abortive coiling and absence of mature sperm in the seminal vesicle.

Fig. 6.

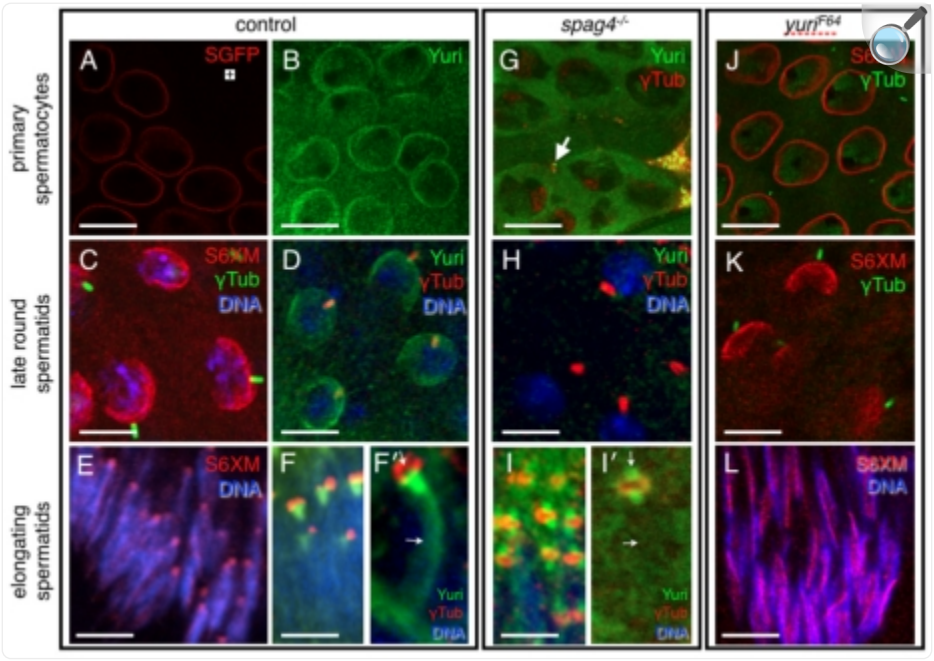

Open in a new tab

Spag4 and Yuri localize to nuclear envelopes, cap, BB dent and stripe during spermatogenesis. Spag4 and Yuri localization at the NE of primary spermatocytes (**A**,**B**), at the centriolar cap on round spermatids (**C**,**D**) and in the BB dent and stripe on elongating nuclei (**E**,**F**) are compellingly similar. **F′** shows Yuri localization on a single elongate nucleus. In the *spag4* mutant, Yuri fails to localize to the NE of primary spermatocytes (**G**) and to the centriolar cap (**H**) and the BB dent and stripe (**I**) at later stages. However, Yuri accumulates on the BB and overlays the CA (I). **I′** also shows absence of Yuri stripe and Yuri accumulation on BB for a single nucleus. Upper arrows in F′, I′ show position of BB, lower arrows show position of stripe. Yuri accumulation on the centrioles of primary spermatocytes is also intermittently seen in the *spag4* mutant (arrow, G). In $yuri^{F64}$, most elements of the Spag4 localization pattern remain (**J**,**K**) but accumulation at the BB dent is lost (**L**). Control genotypes: in A, *w;; spag4:gfp*; in C,E, *w;; spag4:6xmyc*; in B,D,F,F′, w^{1118}. Scale bars 25 μm (A,B,G,J), 15 μm (C,D,H,K), 10 μm (E), 6 μm (F,F′,I,I′,L).

Although Yuri contains neither a transmembrane nor a KASH domain, these data clearly suggest that Spag4 and Yuri are components of the same pathway for centriolar-nuclear association. Furthermore, previous findings for cytoplasmic dynein suggest that it also has a role in this process (Li et al., 2004). Dynein accumulates in the cap pattern on round spermatid nuclei seen for Spag4:6×MYC and Yuri, and loss of this dynein cap in a null mutation of dynein light chain gene *Dlc90F* results in failure of centriole-nucleus association. We therefore investigated the interactions between these

three components further.

Interactions between *spag4*, *yuri* and *dynein* components

As shown above, Spag4 accumulated on the NE of primary spermatocytes, and then decorated the spindle during meiosis. Yuri localization was not determined during these early stages previously (Texada et al., 2008), and was thus investigated as part of this work. We discovered that although Yuri was present on the primary spermatocyte NEs in some spermatocyte cysts (Fig. 6B), it was not present at all stages, suggesting that its presence there is regulated. On round spermatid nuclei, Yuri and Spag4 both formed centriolar caps (Fig. 6C,D), and the proteins colocalized to the stripe and dent in elongating spermatids (supplementary material Fig. S7; Fig. 6E,F,F′).

In contrast to Spag4:6×MYC, Yuri was not detected on the meiotic spindles, and showed diffuse cytoplasmic staining during these divisions. However, Yuri was sometimes detected associated with the centrioles at the NE immediately before meiosis I (data not shown), and routinely Yuri localized to a circumferential ring on the single centrioles at the meiosis II spindle poles (supplementary material Fig. S8). In *spag4*-null flies, Yuri was never detected on the NE of primary spermatocytes, but now could be found on some of the V-shaped centriole pairs at the periphery of these cells (Fig. 6G). No obvious new localization of Yuri emerged during meiosis. But strikingly, the post-meiotic positioning of Yuri relative to the spermatid nuclei and centrioles was dramatically altered in the *spag4* mutant. All elements of the usual nuclear pattern – the cap, dent and stripe – were lost (Fig. 6H,I), and at the onset of nuclear elongation, Yuri began to accumulate ectopically on the dissociating centrioles (Fig. 6I). During elongation, as the centrioles become BBs, the toroid-shaped centriolar adjunct (CA) develops around the rod-like core of the BB (Texada et al., 2008). γ-tubulin is confined to the CA and thus provides an excellent marker for these toroid structures. Using Yuri and γ-tubulin staining, we determined that Yuri not only accumulated on the rod of the BB proper but also frequently coated the outer surface of the CA (Fig. 6I′).

Conversely, in the $yuri^{F64}$ mutant, Spag4:6×MYC accumulation on the primary spermatocyte NEs, the meiotic spindles, and in the cap and stripe remained unaltered (Fig. 6J,K,L). However, one element of the Spag4 distribution pattern was lost: Spag4:6×MYC no longer accumulated at the dent representing the BB attachment site (Fig. 6L). Thus, with the exception of this site, the interactions between the two proteins are very similar to those predicted for a SUN-KASH protein pair.

The effect of loss of the dynein cap at the round spermatid stage (in a *Dlc90F*-null mutant) on the nuclear location of Yuri was reported by Texada and co-workers (Texada et al., 2008). Notably, the effect is similar to that described here upon loss of Spag4: the Yuri cap is strongly reduced, the stripe and dent components never develop, and Yuri accumulates on the BB proper. Thus both *spag4* and dynein have a role in positioning Yuri on the NE. That Yuri has no role in positioning dynein was determined by examining the location of p50:GFP, a tagged subunit of a dynactin, which is a well-established dynein interaction partner (Wojcik et al., 2001). p50:GFP shows identical localization to dynein at

the nucleus and meiotic spindles during spermatogenesis (Li et al., 2004; Anderson et al., 2009), including accumulation in the cap on round spermatid nuclei. In the *yuri*^{F64} mutant, this localization pattern for p50:GFP on the spermatid nuclei remained unchanged (Fig. 7G).

Fig. 7.

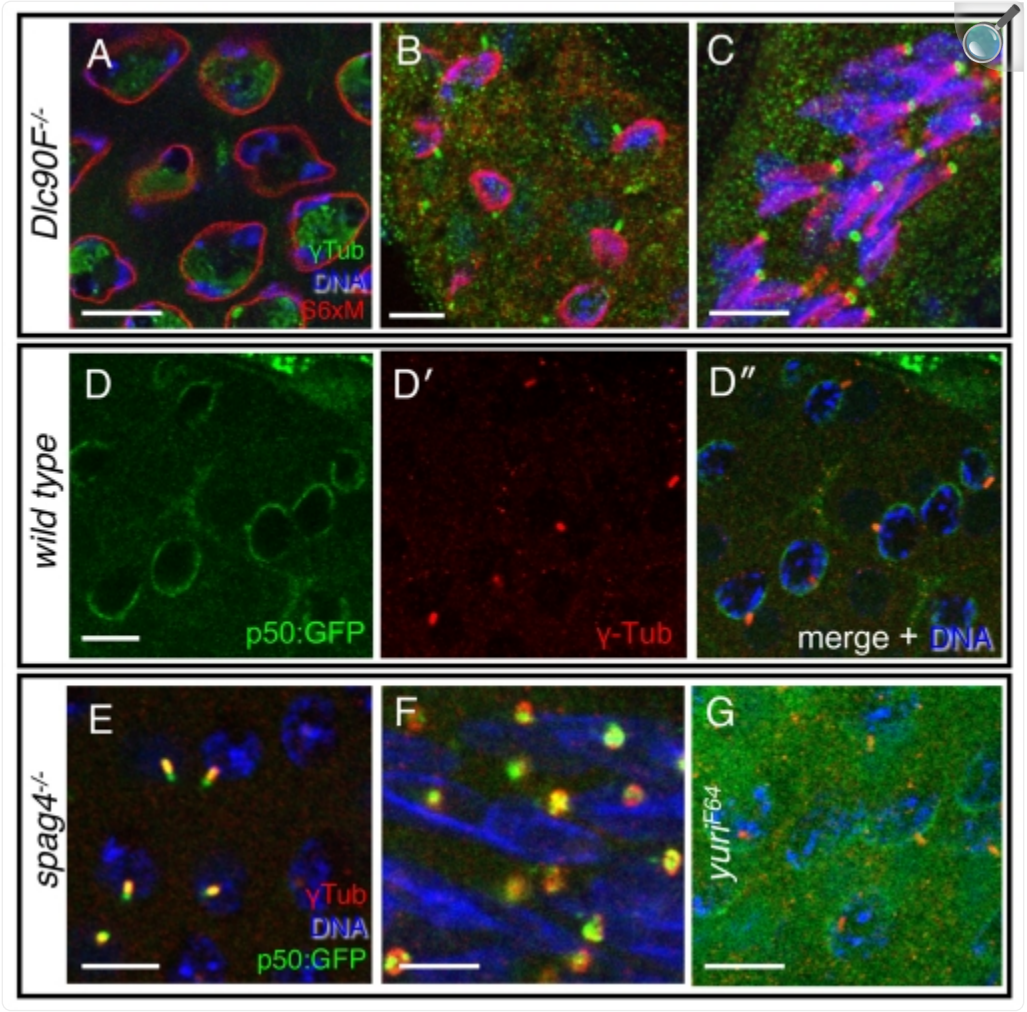

Open in a new tab

Dynein-dynactin components require Spag4, but not Yuri, for localization during spermatogenesis. Spag4:6×MYC localization is essentially normal in (**A**) primary spermatocytes, (**B**) round spermatids and (**C**) elongating spermatids in the *Dlc90F*^{e155} mutant background, although elongating nuclei fail to remain in register. Conversely, the p50:GFP dynactin subunit, which localizes to the centriolar cap on wild-type round spermatid nuclei (**D-D″**), fails to localize normally in the *spag4*-null mutant, aggregating instead on centrioles on round spermatid nuclei (**E**) and in puncta on the CAs of elongating nuclei (**F**). (**G**) Localization of p50:GFP to the centriolar cap is unaffected in the *yuri*^{F64} mutant. Scale bars: 25 μm (A), 10 μm (B-D′,F,G), 8 μm (E).

Throughout spermatogenesis, Spag4:6×MYC localization was unaffected in the *Dlc90F*^{e155}-null mutant (Fig. 7A-C),

indicating that dynein has no role in Spag4 positioning at the NE. But conversely, results for p50:GFP suggest that *spag4* has a role in the localization of dynein-dynactin both before and after meiosis. In *spag4*-null primary spermatocytes, p50:GFP accumulation at the nuclear membrane was lost and instead, similarly to localization of Yuri, p50:GFP accumulated on the paired centrioles at the spermatocyte periphery (data not shown). Likewise, p50:GFP was not detected in the hemispherical cap on round spermatids in *spag4*-null flies, but again, similarly to Yuri in the *spag4* mutant background, accumulated on the BB (Fig. 7E), However, at this stage, the p50:GFP accumulation pattern on the BB was distinct from that of Yuri. All of the p50:GFP was associated with the CA torus, upon which it formed a distinctive pattern of dots around the circumference of the structure (Fig. 7F). These findings indicate that Spag4 is required to bring dynein-dynactin to the nuclear membrane, whereas Yuri, by contrast, requires dynein-dynactin for its accumulation there. A pathway in which the order of gene action is *spag4-dynein-dynactin-yuri* is thus in operation. This model suggests that Spag4 and dynein-dynactin, and Yuri and dynein-dynactin should be simultaneously present at the nuclear surface. Colocalization studies established that these pairs of proteins and all three components together could be detected simultaneously on primary spermatocyte and round spermatid nuclei (supplementary material Fig. S9).

Discussion

Spag4 functions independently of a LINC complex

In this study, we describe the role of Spag4, a *Drosophila* SUN protein. Spag4 is primarily required for linking the centriole and later the BB, two forms of the MTOC of the spermatid, to the nucleus of the elongating spermatid during spermatogenesis. In other contexts, KASH proteins are the essential partners of SUN proteins, forming LINC complexes that tether centrosomes to the NE. However, in single and double mutants of the two KASH protein genes of *Drosophila* lacking the KASH domain, centriole attachment to the spermatid nucleus is normal. Thus Spag4 appears to mediate this interaction by a mechanism that does not involve a typical LINC complex. Consistent with this notion, we have found that Spag4 localization on elongated spermatid nuclei is independent of lamin (supplementary material Fig. S10D), which in other contexts is essential for NE localization of LINC complexes. *Dictyostelium discoideum* cells lack a nuclear lamina, and the SUN protein Sun-1 is thought to interact with chromatin directly (Xiong et al., 2008). Mature sperm also lack a normal nuclear lamina, suggesting that Spag4 might also directly link to chromatin. These unusual features of Spag4 might partly reflect the highly specialized centriole-nuclear interaction that it facilitates. As the *Drosophila* spermatid centriole differentiates into the BB, complex structural rearrangements occur, followed in the final stages by altered relative positioning of the BB and the nucleus (Tokuyasu, 1974; Tokuyasu, 1975).

Spag4 and Yuri are components of a postmeiotic pathway for maintaining the centriole at the spermatid nucleus

In contrast to the KASH proteins, our studies have identified the coiled-coil protein Yuri as an essential component of the postmeiotic Spag4 centriole-tethering pathway. In the post-meiotic stages, Yuri shows identical nuclear positioning to Spag4, and Spag4 is essential for localization of Yuri to its various nuclear sites. These observations place Yuri downstream of Spag4 in the pathway. However, at the nuclear dent, in which the BB sits, there is mutual dependence between the two proteins for correct localization.

In addition to this post-meiotic pathway, a pre-meiotic mechanism exists to bring the centriole pairs of the primary spermatocyte to the NE for function in meiosis. The gene *asunder* (*asun*) is required for this process, which involves accumulation of Asun itself, and Asun-dependent accumulation of dynein (and p50:GFP) at the primary spermatocyte NE (Anderson et al., 2009). As we show here, both Spag4 and Yuri also associate with the primary spermatocyte NE, with localization of Yuri there being Spag4-dependent. However, in contrast to an *asun* mutant, no defects in meiosis were found in $yuri^{F64}$ or *spag4*-null spermatocytes. Thus, no immediate role for the two proteins in pre-meiotic centriole-nuclear association can be postulated. During meiosis, Spag4 is associated with the spindle and astral microtubules. Although a role for SUN proteins in tethering telomeres to the NE during meiosis has been described (Ding et al., 2007; Penkner et al., 2007), we could not detect altered telomere distribution in *spag4*-null meiosis (data not shown). The functions of Yuri and Spag4 in these early stages are thus obscure. Association of Spag4 with the spindle could simply represent a storage location.

The interaction of Yuri and Spag4 in relation to nuclear membrane topology

If Spag4 were a typical SUN protein, its transmembrane domain would traverse the INM, placing its C-terminus in the intermembrane space to interact with a KASH-domain protein spanning the ONM. However none of the isoforms of Yuri has either a transmembrane domain or KASH domain, indicating that a direct interaction between the two proteins in the intermembrane space is unlikely. Thus, despite our evidence that the two known *Drosophila* KASH proteins have no role here, it seems likely that some other ONM protein is needed to bring Yuri and Spag4 together. Our findings on the role of cytoplasmic dynein-dynactin also make a direct interaction of Yuri and Spag4 unlikely. The order of gene action in the pathway appears to be *spag4–dynein-dynactin–yuri*, again probably precluding a direct Spag4-Yuri interaction.

Given these indications of indirect interaction, it is pertinent to ask where Yuri is localized relative to the NE. Previous EM studies (A. D. Tates, PhD thesis, Leiden University, 1971; Tokuyasu, 1974) have shown that the initial cap component of the dense complex forms in a tight compartment between the nuclear membranes proper and a layer of closely apposed ER tubule. In other tissues, we have established that Yuri shows a strong association with the ER rather than the nuclear membranes per se (Michael J. Texada, Rebecca A. Simonette and William J. Deery, unpublished results). It seems likely therefore that Yuri is not bound to the nuclear membranes, but rather is in close apposition to them through association with the overlying ER. If Spag4 is in the inner nuclear membrane, and Yuri in the overlying ER, several components, including an ONM protein and dynein-dynactin, probably link the two proteins. However,

given its unusual interactions, Spag4 might not reside in the INM and thus fewer intermediates might be in play.

Differing molecular activities at the dent and the stripe

The pathway described above is adequate to address the relationship of Yuri and Spag4 at most elements of their nuclear-localization patterns. However, at the dent, further interactions must be invoked, because at this site, localization of the two proteins is mutually dependent. This role of Yuri in positioning Spag4 is unlikely to involve dynein-dynactin, because Yuri has no effect on the localization of p50:GFP(dynactin) at the nuclear surface. Thus additional molecular interactions must take place. Yuri has three isoforms, and it is possible that at this site, an isoform not active at the other locations is in operation (see further discussion below). Our antibody detects all Yuri isoforms, and thus provides no information on individual isoform location.

The different molecular activities at the dent and stripe might reflect different roles for the proteins at these two locations. The dent is closely associated with the BB, and at this site the two proteins function in centriole retention and maturation. The stripe is far removed from this position, and it has been suggested that it might strengthen the nuclei along their long axes during elongation and chromatin condensation (Tokuyasu, 1974). Consistent with this possibility, in both the *yuri*^{F64} and the *spag4* mutants, the fully elongated nuclei are frequently coiled and distorted along their long axis. The stripe contains microtubules, and interestingly, there is evidence that the stripe microtubules represent a distinct class of structures that do not originate from the BB (Tatsuhiko Noguchi, unpublished results).

Similarities to the SUN1-ZYG-12 interaction pair – different roles for Yuri isoforms?

In some ways Yuri is comparable with the KASH protein ZYG-12, which tethers the centrosome to the nucleus in the *Caenorhabditis elegans* zygote by a mechanism involving dynein (Malone et al., 2003). Similarly to Yuri, ZYG-12 is a coiled-coil protein with three isoforms. Furthermore, the longer isoforms of Yuri contain a ~127 residue region with 24% identity and 46% similarity to the ZYG-12 isoforms (supplementary material Fig. S1B). The ZYG-12A isoform localizes to the centrosome, and the B and C isoforms localize to the NE. Direct interaction of the B and C isoforms with dynein leads to close association of the centrosome and nucleus, dimerization of B and C with the A variant, and formation of a stable centrosome-nucleus link. We detected association of Yuri with the centrioles during meiosis II, that is, immediately before Yuri begins to function in maintenance of post-meiotic centriole-nuclear attachment (supplementary material Fig. S8). Furthermore, we identified a role for dynein-dynactin in association of Yuri with the nuclear surface. Given these parallels with ZYG-12, it seems possible that the Yuri isoforms might show differential localization between the centriole and the nuclear surface, and that some Yuri isoforms interact directly with dynein. The overall similar behavior of p50:GFP and Yuri in the *spag4* mutant supports the hypothesis of direct interaction with dynein, but at the same time indicates that Yuri is not directly associated with the dynactin component per se, because the precise localizations of Yuri and p50:GFP on the developing BB in the *spag4*-null mutant are distinctly different

(compare Fig. 6I,I′ and Fig. 7F).

Successful sperm individualization correlates with maintenance of the BB-nucleus link and with properly shaped and bundled elongated nuclei

Mutations in *yuri* and *spag4* result in dissociation of BBs from spermatid nuclei, subsequent curling of the elongate nuclei and finally, failure of individualization. Although BB behavior has not been examined for a mutation to Pros-α6T (a testis-specific proteasome subunit), nevertheless, curled, mislocalized spermatid nuclei are found in this mutant along with aberrant actin cone formation and failed individualization (Zhong and Belote, 2007). Therefore, results for *spag4, yuri* and *Pros-α6T* suggest that dissociation of BB from the nuclei and/or contortion of elongated nuclei correlate with failed IC formation and progression.

How BB detachment from nuclei and nuclear contortion would affect formation of individual actin cones and progression of the IC is not apparent. One possibility is that components of the dense complex at the cap and/or stripe are requisite precursors for formation of actin cones. Actin cone formation begins with the deposition of F-actin filaments along the long axis of the nuclei (Noguchi et al., 2008). The dense complex materials at the cap and the stripe contain F-actin, and this F-actin is lost in $yuri^{F64}$ (Texada et al., 2008). EM examination of the formation of F-actin filaments on the final nuclei of the *spag4,* $yuri^{F64}$ and *Pros-α6T* mutants would address this issue. The male sterile mutation *ms(3)72D* also produces contorted spermatid nuclei (Castrillon et al., 1993) and might thus also be defective in BB-nuclear attachment, actin cone and IC formation, and sperm individualization.

In summary, we have identified Spag4 as a component of a centriolar-nuclear attachment pathway in spermatogenesis that also requires the coiled-coil protein Yuri and cytoplasmic dynein-dynactin. Although Spag4 is a SUN protein, its action in this pathway appears not to involve a conventional KASH protein. The disruption of the later stages of spermatogenesis in *yuri* and *spag4* mutants might be secondary to the general disruption of events at the spermatid nuclear surface produced in these mutants.

Materials and Methods

Drosophila stocks

Transgenic lines were prepared by standard methods at UT Austin or at Genetic Services (Sudbury, MA). Standard genetic crosses were used to introduce: (1) transgenes *pC4-spag4, pC4-spag4:gfp, pC4-spag4:6xmyc, pC4-spag4-SUNstop* and *p50:GFP* into the background of *spag4*-knockout allele #6 and (2) *pC4-spag4:6xmyc* and *p50:GFP* into the $yuri^{F64}$ background. *p50:GFP* and $Dlc90F^{e155}$*/TMB Tb* were obtained from Thomas Hays, University of Minnesota, MN, USA. *w,* α*Tub:gfp, w, yfp:asl* lines (Rebollo et al., 2004; Varmark et al., 2007) and the deficiency spanning *spag4*

Df(2L)Prl, were obtained from Cayetano Gonzalez, Institute for Research and Biomedicine, Barcelona, Spain and the *Drosophila* Stock Center (Bloomington), respectively.

Molecular biology

Molecular biology manipulations were performed using standard techniques. Unless specified, SuperScript II RT reagents and Platinum PCR Supermix (Invitrogen, Carlsbad, CA) were used, and primers from Integrated DNA Technologies (Coralville, IA). Primer sequences are provided in supplementary material Fig. S2. DNA sequencing was performed at the UT Austin ICMB Core Facility.

Expression analysis of *spag4*

Total RNA from ten male or female larvae, pupae and adults was isolated and treated with DNase I, as described (Kracklauer et al., 2007). RT was performed using an oligo (dT) primer followed by PCR with primers P1 and P2.

Determination of *spag4* cDNA ends by RACE

RT-PCR was carried out using male pupal total RNA isolated as recommended in the FirstChoice RLM-RACE kit protocol (Ambion, Austin, TX), and then used in 5′ RLM-RACE and 3′ RACE. The 5′ end of the gene was amplified using the RNA adapter-specific forward outer and inner primers, and the gene-specific reverse primer P3. To amplify the 3′ end of the gene, anchored oligo-(dT) adapter primers from the FirstChoice kit were used in RT. In the PCR, the gene-specific forward primer P4 and the 3′ adapter-specific outer primer were used. 5′ and 3′ RACE products were subcloned into pGEM-T-Easy (Promega, Madison, WI) and their sequences verified. A complete *spag4* cDNA with 5′ and 3′ UTRs was generated by PCR using a mixture of partially overlapping RACE products as template and the 5′ and 3′ adapter-specific primers. The final PCR product was subcloned into pGEM-T-Easy, sequenced and catalogued as EF537040 at NCBI.

Construction of *spag4* genomic transgenes

The transgene *pC4-spag4* was generated by ligating the *spag4* coding region as a 4.9 kb *Pst*I fragment from *BACR02J20* into the *Pst*I site of *pCaSpEr-4* (pC4) (Thummel and Pirrotta, 1992). The GFP-tagged version, *pC4-spag4*:*gfp,* was generated by ligating the GFP ORF from *pUAST-gfp* (Kracklauer et al., 2007) immediately downstream of the *spag4* coding region in *pC4-spag4*. For this purpose, an *Asc*I site was introduced immediately upstream of the *spag4* stop codon using the QuikChange II PCR Mutagenesis Kit (Stratagene) and primer pair P13-P14. The GFP ORF with *Asc*I sites on both ends (generated by PCR using primers P11-P12 on the *pUAST-gfp* template) was then cloned into this *Asc*I site. To generate *pC4-spag4*:*6xmyc*, a *6xmyc* ORF was amplified from the *pUAST-6xmyc* vector (Kracklauer et al., 2007)

using the PCR primers P15 and P16, and the ORF was then cloned into the *Asc*I site as for *pC4-spag4*:*GFP*. To generate *pC4-spag4*^{SUNstop}, a stop codon was introduced into the 4.9 kb *Pst*I fragment using the mutagenic primers P21-P22, and the resulting mutated fragment was cloned into the *Pst*I site of *pC4* as described above.

Generation of *spag4* knockout

The targeting construct (*pW35-spag4*^{HRKO}) was generated as follows. DNA sequences of ~3 kb (upstream) and ~5 kb (downstream) flanking the *spag4* coding region were amplified by PCR using hot-start Herculase (Stratagene, La Jolla, CA), primer sets P5-P6 and P7-P8, and *BAC02J20* (Open Biosystems, Huntsville, AL) as template. PCR products were subcloned into pGEM-T-Easy and their sequences verified. The upstream 3 kb fragment was excised from pGEM-T-Easy with *Not*I and cloned into that site of *pW35* (Gong and Golic, 2003). The downstream 5 kb fragment was excised from pGEM-T-Easy with *Bam*HI and *Avr*II, then cloned into those sites in *pW35* downstream of the w^+ marker gene, resulting in *pW35-spag4*^{HRKO}. After generation of transgenic lines, a cross of 500 *y w, pW35 spag4*^{HRKO}*/FM7c, gfp* virgin females with 500 *(y) w;; [hs-FLP],[hs-I-SceI]/TM3, Sb* males was set up with subsequent embryo manipulation and heat shocks, as described previously (Kracklauer et al., 2007). ~400 crosses of 3-4 w^+-mosaic *(y) w, pW35-spag4*^{HRKO}*/+;; [hs-FLP],[hs-I-SceI]/+* F1 virgin females and 3-4 *w; hs-FLP* males were performed. F2 progeny were screened for a single male from each cross with solid w^+ eyes, indicative of targeted insertion events. Insertions were mapped for 100 independent F2 candidate knockout males using standard methods; for 87 candidates, the insertion mapped to chromosome 2 as expected. For ~50 such stocks, *spag4* targeting was assessed by Southern blotting (Kracklauer et al., 2007). Ultimately, five independent *spag4* knockout alleles – 1, 6, 11, 12 and 15 – were isolated. Allele 6 was used for most studies.

Quantitative fertility assays

Twenty individual *spag4* homozygous *or spag4/Df(2L)Prl* males were each crossed to two w^{1118} virgins. As a control, 20 crosses using w^{1118} males homozygous for a wild-type (Oregon-R) copy of chromosome 2 (w^{1118}*;ORC2*^{iso}) were set up. For the fertility rescue assays, 20 individual *spag4* homozygous males bearing a single copy of the transgene *pC4-spag4*, *pC4-spag4*:*gfp*, *pC4-spag4*:*6xmyc* or *pC4-spag4-SUNstop* were used. To assay female fertility, 20 virgin *spag4* homozygous or *spag4/Df(2L)Prl* females were assayed individually with two w^{1118} males. Similar crosses with w^{1118}*; ORC2*^{iso} virgin females were set up in parallel as wild-type controls. After 1 week, average combined numbers of larvae and pupae per vial were determined.

TEM

Testes were fixed on ice for 2 hours in PBS with 2% glutaraldehyde [Electron Microscopy Sciences (EMS), Hatfield, PA], rinsed, then post-fixed at room temperature for 2 hours in 2% OsO_4 (EMS) and 0.8% $K_3[Fe(CN)_6]$ in 1×

symcollidine buffer (McDonald, 1984; Jinguji and Ishikawa, 1990). Tissues were then dehydrated and embedded in resin using standard procedures. 50-60 nm sections were cut, stained with uranyl acetate and lead citrate and examined with a Philips EM208 electron microscope.

Immunocytology

Testes were fixed and stained essentially as described (Lin et al., 1996; Zhong and Belote, 2007; Texada et al., 2008), and mounted in VectaShield (Vector Laboratories, Burlingame, CA) or 50% glycerol. Primary antibody dilutions were as follows: mouse anti-MYC, 1:2000; rabbit anti-MYC, 1:200; rabbit anti-CM1, 1:100 (all from Cell Signaling Technology, Danvers, MA); rabbit anti-Vasa, 1:200 (Santa Cruz Biotechnology, Santa Cruz, CA); mouse anti-γ-tubulin, 1:500 (Sigma) and chicken anti-Yuri, 1:400 (Texada et al., 2008). Secondary antibodies were Alexa Fluor 488 anti-rabbit, Alexa Fluor 555 or Alexa Fluor 568 anti-mouse and Alexa Fluor 488 anti-chicken, all at 1:500 (Invitrogen). Alexa Fluor phalloidin (Invitrogen) to stain F-actin and TOPRO-3 to stain DNA, were mixed into secondary antibody solutions at 15 µl phalloidin/ml and 1 µl/ml TOPRO-3. DAPI for DNA staining was added to mounting solution at 1 µl/ml. Testes were imaged with Leica AOBS SP2 and Zeiss LSM 510 laser-scanning confocal microscopes and a Zeiss Axioplan microscope using Metamorph deconvolution software. Adobe Photoshop was used to process all images.

In situ hybridization (ISH)

ISH was carried out essentially as described (White-Cooper et al., 1998), using an 820 bp PCR product from the *spag4* ORF to generate sense and antisense probes by in vitro transcription with a DIG RNA Labeling Kit (Roche).

Supplementary Material

[Supplementary Material]

supp_123_16_2763__index.html (6.6KB, html)

Acknowledgments

We are grateful to C. Schmidt for critically reviewing this manuscript, to Y. Yamashita for support, to C. Gonzalez and T. Hays for providing flies and reagents, and to K. Lea for assistance with generating the *pW35-spag4*^{HRKO} construct. This work was supported by a grant from the National Eye Institute (RO1-EY13958) to J.A.F and grants C-1119 from

the Welch Foundation of Texas and NNX09AH43G from NASA to K.M.B. Deposited in PMC for release after 12 months.

Footnotes

Supplementary material available online at http://jcs.biologists.org/cgi/content/full/123/16/2763/DC1

References

1. Anderson M. A., Jodoin J. N., Lee E., Hales K. G., Hays T. S., Lee L. A. (2009). Asunder is a critical regulator of dynein-dynactin localization during Drosophila spermatogenesis. *Mol. Biol. Cell* 20, 2709-2721 [DOI] [PMC free article] [PubMed] [Google Scholar]

2. Arama E., Steller H. (2006). Detection of apoptosis by terminal deoxynucleotidyl transferase-mediated dUTP nick-end labeling and acridine orange in Drosophila embryos and adult male gonads. *Nat. Protoc.* 1, 1725-1731 [DOI] [PubMed] [Google Scholar]

3. Arama E., Agapite J., Steller H. (2003). Caspase activity and a specific cytochrome C are required for sperm differentiation in Drosophila. *Dev. Cell* 4, 687-697 [DOI] [PubMed] [Google Scholar]

4. Armstrong J. D., Texada M. J., Munjaal R., Baker D. A., Beckingham K. M. (2006). Gravitaxis in Drosophila melanogaster: a forward genetic screen. *Genes Brain Behav.* 5, 222-239 [DOI] [PubMed] [Google Scholar]

5. Bray J. D., Chennathukuzhi V. M., Hecht N. B. (2002). Identification and characterization of cDNAs encoding four novel proteins that interact with translin associated factor-X. *Genomics* 79, 799-808 [DOI] [PubMed] [Google Scholar]

6. Castrillon D. H., Gonczy P., Alexander S., Rawson R., Eberhart C. G., Viswanathan S., DiNardo S., Wasserman S. A. (1993). Toward a molecular genetic analysis of spermatogenesis in Drosophila melanogaster: characterization of male-sterile mutants generated by single P element mutagenesis. *Genetics* 135, 489-505 [DOI] [PMC free article] [PubMed] [Google Scholar]

7. Crisp M., Liu Q., Roux K., Rattner J. B., Shanahan C., Burke B., Stahl P. D., Hodzic D. (2006). Coupling of the nucleus and cytoplasm: role of the LINC complex. *J. Cell Biol.* 172, 41-53 [DOI] [PMC free article] [PubMed] [Google Scholar]

8. Ding X., Xu R., Yu J., Xu T., Zhuang Y., Han M. (2007). SUN1 is required for telomere attachment to

nuclear envelope and gametogenesis in mice. *Dev. Cell* 12, 863-872 [DOI] [PubMed] [Google Scholar]

9. Dreger M., Bengtsson L., Schoneberg T., Otto H., Hucho F. (2001). Nuclear envelope proteomics: novel integral membrane proteins of the inner nuclear membrane. *Proc. Natl. Acad. Sci. USA* 98, 11943-11948 [DOI] [PMC free article] [PubMed] [Google Scholar]

10. Fischer J. A., Acosta S., Kenny A., Cater C., Robinson C., Hook J. (2004). Drosophila Klarsicht has distinct subcellular localization domains for nuclear envelope and microtubule localization in the eye. *Genetics* 168, 1385-1393 [DOI] [PMC free article] [PubMed] [Google Scholar]

11. Fischer-Vize J. A., Mosley K. L. (1994). Marbles mutants: uncoupling cell determination and nuclear migration in the developing Drosophila eye. *Development* 120, 2609-2618 [DOI] [PubMed] [Google Scholar]

12. Fuller M. T. (1993). Spermatogenesis. In *The Development of Drosophila melanogaster*, Vol. 1 (ed. Bate M., Martinez-Arias A.), pp. 71-147 New York: Cold Spring Harbor Press; [Google Scholar]

13. Gomes E. R., Jani S., Gundersen G. G. (2005). Nuclear movement regulated by Cdc42, MRCK, myosin, and actin flow establishes MTOC polarization in migrating cells. *Cell* 121, 451-463 [DOI] [PubMed] [Google Scholar]

14. Gong W. J., Golic K. G. (2003). Ends-out, or replacement, gene targeting in Drosophila. *Proc. Natl. Acad. Sci. USA* 100, 2556-2561 [DOI] [PMC free article] [PubMed] [Google Scholar]

15. Gruenbaum Y., Margalit A., Goldman R. D., Shumaker D. K., Wilson K. L. (2005). The nuclear lamina comes of age. *Nat. Rev. Mol. Cell Biol.* 6, 21-31 [DOI] [PubMed] [Google Scholar]

16. Guo Y., Jangi S., Welte M. A. (2005). Organelle-specific control of intracellular transport: distinctly targeted isoforms of the regulator Klar. *Mol. Biol. Cell* 16, 1406-1416 [DOI] [PMC free article] [PubMed] [Google Scholar]

17. Hagan I., Yanagida M. (1995). The product of the spindle formation gene sad1+ associates with the fission yeast spindle pole body and is essential for viability. *J. Cell Biol.* 129, 1033-1047 [DOI] [PMC free article] [PubMed] [Google Scholar]

18. Hicks J. L., Deng W. M., Rogat A. D., Miller K. G., Bownes M. (1999). Class VI unconventional myosin is required for spermatogenesis in Drosophila. *Mol. Biol. Cell* 10, 4341-4353 [DOI] [PMC free article] [PubMed] [Google Scholar]

19. Hodzic D. M., Yeater D. B., Bengtsson L., Otto H., Stahl P. D. (2004). Sun2 is a novel mammalian inner nuclear membrane protein. *J. Biol. Chem.* 279, 25805-25812 [DOI] [PubMed] [Google Scholar]

20. Huh J. R., Vernooy S. Y., Yu H., Yan N., Shi Y., Guo M., Hay B. A. (2004). Multiple apoptotic caspase cascades are required in nonapoptotic roles for *Drosophila* spermatid individualization. *PLoS Biol.* 2, E15 [DOI] [PMC free article] [PubMed] [Google Scholar]

21. Jinguji Y., Ishikawa H. (1990). An osmium-ferricyanide staining method for the intercellular space in the small intestinal epithelium. *J. Electron Microsc. (Tokyo)* 39, 59-62 [PubMed] [Google Scholar]

22. Kennedy C., Sebire K., de Kretser D. M., O' Bryan M. K. (2004). Human sperm associated antigen (SPAG4) is a potential cancer marker. *Cell Tissue Res.* 315, 279-283 [DOI] [PubMed] [Google Scholar]

23. Ketema M., Wilhelmsen K., Kuikman I., Janssen H., Hodzic D., Sonnenberg A. (2007). Requirements for the localization of nesprin-3 at the nuclear envelope and its interaction with plectin. *J. Cell Sci.* 120, 3384-3394 [DOI] [PubMed] [Google Scholar]

24. King M. C., Drivas T. G., Blobel G. (2008). A network of nuclear envelope membrane proteins linking centromeres to microtubules. *Cell* 134, 427-438 [DOI] [PMC free article] [PubMed] [Google Scholar]

25. Kracklauer M., Banks S. M. L., Xie X., Wu Y., Fischer J. A. (2007). Drosophila klaroid encodes a SUN domain protein required for Klarsicht localization to the nuclear envelope and nuclear migration in the eye. *Fly* 1, 17-27 [DOI] [PubMed] [Google Scholar]

26. Li M.-G., Serr M., Newman E. A., Hays T. S. (2004). The Drosophila tctex-1 light chain is dispensable for essential cytoplasmic dynein functions but is required during spermatid differentiation. *Mol. Biol. Cell* 15, 3005-3014 [DOI] [PMC free article] [PubMed] [Google Scholar]

27. Lin T. Y., Viswanathan S., Wood C., Wilson P. G., Wolf N., Fuller M. T. (1996). Coordinate developmental control of the meiotic cell cycle and spermatid differentiation in Drosophila males. *Development* 122, 1331-1341 [DOI] [PubMed] [Google Scholar]

28. Liu Q., Pante N., Misteli T., Elsagga M., Crisp M., Hodzic D., Burke B., Roux K. J. (2007). Functional association of Sun1 with nuclear pore complexes. *J. Cell Biol.* 178, 785-798 [DOI] [PMC free article] [PubMed] [Google Scholar]

29. Lüke Y., Zaim H., Karakesisoglou I., Jaeger V. M., Sellin L., Lu W., Schneider M., Neumann S., Beijer A., Munck M., et al. (2008). Nesprin-2 Giant (NUANCE) maintains nuclear envelope architecture and composition in skin. *J. Cell Sci.* 121, 1887-1898 [DOI] [PubMed] [Google Scholar]

30. Malone C. J., Fixsen W. D., Horvitz H. R., Han M. (1999). UNC-84 localizes to the nuclear envelope and is required for nuclear migration and anchoring during C. elegans development. *Development* 126, 3171-3181 [DOI] [PubMed] [Google Scholar]

31. Malone C. J., Misner L., Le Bot N., Tsai M. C., Campbell J. M., Ahringer J., White J. G. (2003). The C.

elegans hook protein, ZYG-12, mediates the essential attachment between the centrosome and nucleus. *Cell* 115, 825-836 [DOI] [PubMed] [Google Scholar]

32. McDonald K. (1984). Osmium ferricyanide fixation improves microfilament preservation and membrane visualization in a variety of animal cell types. *J. Ultrastruct. Res.* 86, 107-118 [DOI] [PubMed] [Google Scholar]

33. McGee M. D., Rillo R., Anderson A. S., Starr D. A. (2006). UNC-83 IS a KASH protein required for nuclear migration and is recruited to the outer nuclear membrane by a physical interaction with the SUN protein UNC-84. *Mol. Biol. Cell* 17, 1790-1801 [DOI] [PMC free article] [PubMed] [Google Scholar]

34. Mosley-Bishop K. L., Li Q., Patterson L., Fischer J. A. (1999). Molecular analysis of the klarsicht gene and its role in nuclear migration within differentiating cells of the Drosophila eye. *Curr. Biol.* 9, 1211-1220 [DOI] [PubMed] [Google Scholar]

35. Muro I., Berry D. L., Huh J. R., Chen C. H., Huang H., Yoo S. J., Guo M., Baehrecke E. H., Hay B. A. (2006). The Drosophila caspase Ice is important for many apoptotic cell deaths and for spermatid individualization, a nonapoptotic process. *Development* 133, 3305-3315 [DOI] [PubMed] [Google Scholar]

36. Noguchi T., Miller K. G. (2003). A role for actin dynamics in individualization during spermatogenesis in Drosophila melanogaster. *Development* 130, 1805-1816 [DOI] [PubMed] [Google Scholar]

37. Noguchi T., Lenartowska M., Rogat A. D., Frank D. J., Miller K. G. (2008). Proper cellular reorganization during Drosophila spermatid individualization depends up actin structures composed of two domains, bundles and meshwork, that are differentially regulate and have different functions. *Mol. Biol. Cell* 19, 2363-2372 [DOI] [PMC free article] [PubMed] [Google Scholar]

38. Patterson K., Molofsky A. B., Robinson C., Acosta S., Cater C., Fischer J. A. (2004). The functions of Klarsicht and nuclear lamin in developmentally regulated nuclear migrations of photoreceptor cells in the Drosophila eye. *Mol. Biol. Cell* 15, 600-610 [DOI] [PMC free article] [PubMed] [Google Scholar]

39. Penkner A., Tang L., Novatchkova M., Ladurner M., Fridkin A., Gruenbaum Y., Schweizer D., Loidl J., Jantsch V. (2007). The nuclear envelope protein Matefin/SUN-1 is required for homologous pairing in C. elegans meiosis. *Dev. Cell* 12, 873-885 [DOI] [PubMed] [Google Scholar]

40. Rebollo E., Llamazares S., Reina J., Gonzalez C. (2004). Contribution of noncentrosomal microtubules to spindle assembly in Drosophila spermatocytes. *PLoS Biol.* 2, E8 [DOI] [PMC free article] [PubMed] [Google Scholar]

41. Shao X., Tarnasky H. A., Lee J. P., Oko R., van der Hoorn F. A. (1999). Spag4, a novel sperm protein,

binds outer dense-fiber protein Odf1 and localizes to microtubules of manchette and axoneme. *Dev. Biol.* 211, 109-123 [DOI] [PubMed] [Google Scholar]

42. Starr D. A., Han M. (2002). Role of ANC-1 in tethering nuclei to the actin cytoskeleton. *Science* 298, 406-409 [DOI] [PubMed] [Google Scholar]

43. Starr D. A., Fischer J. A. (2005). KASH'n Karry: the KASH domain family of cargospecific cytoskeletal adaptor proteins. *BioEssays* 27, 1136-1146 [DOI] [PubMed] [Google Scholar]

44. Starr D. A., Hermann G. J., Malone C. J., Fixsen W., Priess J. R., Horvitz H. R., Han M. (2001). unc-83 encodes a novel component of the nuclear envelope and is essential for proper nuclear migration. *Development* 128, 5039-5050 [DOI] [PubMed] [Google Scholar]

45. Stewart-Hutchinson P. J., Hale C. M., Wirtz D., Hodzic D. (2008). Structural requirements for the assembly of LINC complexes and their function in cellular mechanical stiffness. *Exp. Cell Res.* 314, 1892-1905 [DOI] [PMC free article] [PubMed] [Google Scholar]

46. Texada M. J., Simonette R. A., Johnson C. B., Deery W. J., Beckingham K. M. (2008). Yuri gagarin is required for actin, tubulin and basal body functions in Drosophila spermatogenesis. *J. Cell Sci.* 121, 1926-1936 [DOI] [PubMed] [Google Scholar]

47. Thummel C. S., Pirrotta V. (1992). Technical notes: new pCasper P-element vectors. *Dros. Inf. Serv.* 71, E150 [Google Scholar]

48. Tokuyasu K. T. (1974). Dynamics of spermiogenesis in Drosophila melanogaster. IV. Nuclear transformation. *J. Ultrastruct. Res.* 48, 284-303 [DOI] [PubMed] [Google Scholar]

49. Tokuyasu K. T. (1975). Dynamics of spermiogenesis in Drosophila melanogaster. V. Head-tail alignment. *J. Ultrastruct. Res.* 50, 117-129 [DOI] [PubMed] [Google Scholar]

50. Tweedie S., Ashburner M., Falls K., Leyland P., McQuilton P., Marygold S., Millburn G., Osumi-Sutherland D., Schroeder A., Seal R., et al. (2009). FlyBase: enhancing Drosophila gene ontology annotations. *Nucleic Acids Res.* 37, D555-D559 [DOI] [PMC free article] [PubMed] [Google Scholar]

51. Varmark H., Llamazares S., Rebollo E., Lange B., Reina J., Schwarz H., Gonzalez C. (2007). Asterless is a centriolar protein required for centrosome function and embryo development in Drosophila. *Curr. Biol.* 17, 1735-1745 [DOI] [PubMed] [Google Scholar]

52. White-Cooper H., Schafer M. A., Alphey L. S., Fuller M. T. (1998). Transcriptional and post-transcriptional control mechanisms coordinate the onset of spermatid differentiation with meiosis I in Drosophila. *Development* 125, 125-134 [DOI] [PubMed] [Google Scholar]

53. Wilhelmsen K., Litjens S. H., Kuikman I., Tshimbalanga N., Janssen H., van den Bout I., Raymond K., Sonnenberg A. (2005). Nesprin-3, a novel outer nuclear membrane protein, associates with the cytoskeletal linker protein plectin. *J. Cell Biol.* 171, 799-810 [DOI] [PMC free article] [PubMed] [Google Scholar]

54. Wojcik E., Basto R., Serr M., Scaerou F., Karess R., Hays T. (2001). Kinetochore dynein: its dynamics and role in the transport of the Rough deal checkpoint protein. *Nat. Cell Biol.* 3, 1001-1007 [DOI] [PubMed] [Google Scholar]

55. Xie X., Fischer J. A. (2008). On the roles of the Drosophila KASH domain proteins MSP-300 and Klarsicht. *Fly* 2, 1-8 [DOI] [PubMed] [Google Scholar]

56. Xiong H., Rivero F., Euteneuer U., Mondal S., Mana-Capelli S., Larochelle D., Vogel A., Gassen B., Noegel A. A. (2008). Dictyostelium Sun-1 connects the centrosome to chromatin and ensures genome stability. *Traffic* 9, 708-724 [DOI] [PubMed] [Google Scholar]

57. Zhang Q., Ragnauth C., Greener M. J., Shanahan C. M., Roberts R. G. (2002). The nesprins are giant actin-binding proteins, orthologous to Drosophila melanogaster muscle protein MSP-300. *Genomics* 80, 473-481 [PubMed] [Google Scholar]

58. Zhong L., Belote J. M. (2007). The testis-specific proteasome subunit Prosalpha6T of *D. melanogaster* is required for individualization and nuclear maturation during spermatogenesis. *Development* 134, 3517-3525 [DOI] [PubMed] [Google Scholar]

Associated Data

This section collects any data citations, data availability statements, or supplementary materials included in this article.

Supplementary Materials

[Supplementary Material]

supp_123_16_2763__index.html (6.6KB, html)

supp_123_16_2763__1.pdf (132KB, pdf)

supp_123_16_2763__10.pdf (30.8KB, pdf)

supp_123_16_2763__2.pdf (23KB, pdf)

supp_123_16_2763__3.pdf (4MB, pdf)

supp_123_16_2763__4.pdf (359.1KB, pdf)

supp_123_16_2763__5.pdf (680.3KB, pdf)

supp_123_16_2763__6.pdf (697.3KB, pdf)

supp_123_16_2763__7.pdf (630.4KB, pdf)

supp_123_16_2763__8.pdf (469KB, pdf)

supp_123_16_2763__9.pdf (594.3KB, pdf)